Normalized Optimal Control Modification and Flight Experiments on NASA F/A-18 Aircraft

Nhan Nguyen*

NASA Ames Research Center, Moffett Field, CA 94035

Curtis Hanson†

NASA Armstrong Flight Research Center, Edwards, CA 93523

John Burken‡

NASA Armstrong Flight Research Center, Edwards, CA 93523

Jacob Schaefer§

NASA Armstrong Flight Research Center, Edwards, CA 93523

I. Introduction

It is well-known that the use of a large adaptive gain in model-reference adaptive control (MRAC) can result in poor robustness.[1] Two well-known robust modification methods, namely; the σ-modification[2] and e-modification,[3] have been used extensively. The last decade has seen a surge in many new adaptive control methods such as the $\mathscr{L}_1$ adaptive control,[4] adaptive loop transfer recovery,[5] Kalman filter adaptive control,[32] derivative-free adaptive control,[7] composite model-reference adaptive control,[8] optimal control modification,[9] and others.

The optimal control modification was developed in 2008 based on an optimal control framework.[9,10] For linear uncertain plants, the optimal control modification can be shown to have a linear asymptotic property for fast adaptation.[11–13] This allows stability properties of the optimal control modification to be analyzed for asymptotic linear plants in the limit. Using this approach, the Rohrs counterexample has been successfully redesigned with the optimal control modification to provide an analytical stability margin in the limit.[11] Maintaining fast adaptation even after the

*Research Scientist, Intelligent Systems Division, Mail Stop 269-1, AIAA Associate Fellow
†Aerospace Engineer, Flight Controls Branch, P.O. Box 273/Mail Stop 4840D, AIAA Member
‡Aerospace Engineer, Flight Controls Branch, P.O. Box 273/Mail Stop 4840D, AIAA Senior Member
§Aerospace Engineer, Flight Controls Branch, P.O. Box 273/Mail Stop 4840D, AIAA Member

adaptation has achieved its objective can result in persistent learning which would do little to further improve tracking performance. Persistent learning may also reduce robustness. Therefore, the optimal control modification has been developed to enable the adaptive gain to be adjusted by a covariance-like update law.[14] The adjustment allows a large initial adaptive gain to be used to reduce the initial transients. The covariance update law then adjusts the adaptive gain toward a lower value as the adaptation continues, thereby achieving desired improved robustness while retaining tracking performance. While the covariance adjustment is used extensively in recursive least-squares (RLS) methods,[15] it is not typically used in the standard MRAC since the stability proof of this adjustment mechanism is generally more difficult. Narendra proposes an output feedback control with time-varying gains based on a least squares method for a time-dependent input function.[16] In general, if the input function is an explicit function of time, then the estimation error tends to zero exponentially if the persistent excitation (PE) condition is met. Unlike least-squares methods, the complex dynamics from the covariance adjustment with a state-dependent input function in the standard MRAC does not provide bounds on adaptive parameters. One way to avoid this difficulty is to use the projection method. In this work, the stability proof of the covariance adjustment can easily be established with the optimal control modification in the context of MRAC based on the tracking error and can be shown to provide theoretical bounds on the modification and adjustment parameters to guarantee stability for a given a priori uncertainty bound. In contrast, the covariance update in RLS is usually defined without any adjustment parameter. This feature distinguishes this method from the least-squares methods. Furthermore, it can be used without the projection method since the optimal control modification ensures boundedness of adaptive parameters.

Stability of adaptive control is known to be sensitive to the amplitude of an input function. This effect can be reduced by the normalization to improve robustness. Normalized MRAC has been studied by a number of researchers. Ioannu develops extensive normalization methods for least-squares methods.[15] For simple first-order systems, Ioannu proposes a least-squares adaptive control which employs a modified estimation error signal with a normalized term in order to avoid the complication of system dynamics.[15] This results in a modified tracking error equation but the tracking error is not available for the adaptive law.[15] Another modified error signal is studied by Ioannu whereby the output error is divided by the normalization factor for output feedback control using an input function which is a first-order filter of the state variable.[15] Similarly, Narendra also studies the normalization for output feedback control based on a least-squares method using a modified output error signal that includes an auxiliary error signal.[16] Boskovic proposes normalized least-squares adaptive laws[17] that include a static observer and alternatively a dynamic observer using the state and control information passed through a first-order filter. The normalized adaptive laws are then used with the projection in least-squares adaptive control. Åström and Wittenmark propose normalized σ-modification and e-modification that explicitly include a priori bounds on adaptive parameters.[18] In this work, a new stability proof for the normalized optimal control modification in the context of MRAC based on the tracking error is presented that does not rely on the projection or any modification of the error signals. The stability proof provides a new way of finding

an ultimate bound to handle the complex normalization factor.

Flight control simulations demonstrate that both covariance adjustment and normalization for the optimal control modification improve performance and robustness. NASA Armstrong Flight Research Center conducted a series of flight experiments onboard a NASA F/A-18 aircraft to evaluate three adaptive control methods with varying complexity.[19] The normalized optimal control modification was implemented as two of the adaptive controllers along with a simple MRAC. The flight experiments were designed to investigate the effectiveness of a simple MRAC design and the potential performance benefits with a more complex MRAC design. The flight test results show that the adaptive controllers can effectively restore the aircraft performance in the presence of failures. The normalized optimal control modification was shown to be able to provide improved performance under a number of failures. The flight test results indicate the potential benefit of the normalized optimal control modification.

II. Optimal Control Modification with Covariance Adjustment

Let a nonlinear plant with a matched uncertainty and an unmatched disturbance be given as

$$\dot{x} = Ax + B\left[u + \Theta^{*\top}\Phi(x)\right] + w \tag{1}$$

where $x(t) : [0,\infty) \to \mathbb{R}^n$ is a state vector, $u(t) : [0,\infty) \to \mathbb{R}^p$ is a control vector, $A \in \mathbb{R}^{n\times n}$ and $B \in \mathbb{R}^{n\times p}$ are known such that the pair (A,B) is controllable, $\Theta^* \in \mathbb{R}^{m\times p}$ is an unknown constant ideal weight matrix that represents a parametric uncertainty, $\Phi(x) : \mathbb{R}^n \to \mathbb{R}^m$ is a vector of known input functions that are continuous and at least in $\mathscr{C}^1$, and $w(t) : [0,\infty) \to \mathbb{R}^n$ is a bounded disturbance with an upper bound w_0 such that $\sup_{\forall t} \|w\| \leq w_0$.

A feedback adaptive control $u(t)$, to achieve a command-following objective, is designed as

$$u = -K_x x + K_r r - u_{ad} \tag{2}$$

where $r(t) : [0,\infty) \to \mathbb{R}^p \in \mathscr{L}_\infty$ is a bounded command vector, $K_x \in \mathbb{R}^{p\times n}$ is a stable feedback gain matrix such that $A - BK_x$ is Hurwitz, $K_r \in \mathbb{R}^{p\times p}$ is a feedforward gain matrix, and $u_{ad}(t) : [0,\infty) \to \mathbb{R}^p$ is an adaptive signal given by

$$u_{ad} = \Theta^\top \Phi(x) \tag{3}$$

where $\Theta(t) : [0,\infty) \to \mathbb{R}^{m\times p}$ is an estimate of the parametric uncertainty Θ^*.

Let $A_m = A - BK_x$ and $B_m = BK_r$. The reference model is established as

$$\dot{x}_m = A_m x_m + B_m r \tag{4}$$

Let $\tilde{\Theta} = \Theta - \Theta^*$ be an estimation error and $e = x_m - x$ be the tracking error. Then the tracking error dynamics are described by

$$\dot{e} = A_m e + B\tilde{\Theta}^\top \Phi(x) - w \tag{5}$$

The optimal control modification adaptive law is established by[9,10]

$$\dot{\Theta} = -\Gamma\Phi(x)\left[e^\top P - \nu\Phi^\top(x)\Theta B^\top P A_m^{-1}\right]B \tag{6}$$

This adaptive law seeks bounded tracking by minimizing the $\mathscr{L}_2$ tracking error norm $\|e\|_2$ bounded away from some unknown lower bound $\Delta(t)$ with the following cost function

$$J = \lim_{t_f\to\infty}\frac{1}{2}\int_0^{t_f}(e-\Delta)^\top Q(e-\Delta)\,dt \tag{7}$$

subject to the tracking error dynamics in Eq. (5), where $Q = Q^\top > 0 \in \mathbb{R}^{n\times n}$ is a positive-definite weighting matrix.

The modification parameter ν provides improved robustness when its value is increased. On the other hand, reducing the value of ν provides improved tracking performance. In the limit when $\nu = 0$, the standard MRAC is recovered and asymptotic tracking performance is achieved but at the expense of robustness, as well-demonstrated by the Rohrs counterexample.[1] By not requiring asymptotic tracking, the adaptation can be made more robust.

Robustness of the optimal control modification can be further improved by the use of a time-varying adaptive gain with a covariance adjustment as follows:

$$\dot{\Gamma} = -\eta\Gamma\Phi(x)\Phi^\top(x)\Gamma \tag{8}$$

where $0 \le \eta < \nu\lambda_{min}\left(B^\top A_m^{-\top} Q A_m^{-1} B\right)$ is an adjustment parameter.

It is important to note that the standard covariance resetting in least-squares methods is defined without the adjustment parameter η. Furthermore, in least-squares methods, the input function is normally a function of time which greatly simplifies the stability proof. In the present method, the adjustment parameter η cannot be arbitrarily chosen and has an upper limit to guarantee stability. Moreover, the input function $\Phi(x)$ depends on the overall stability of the adaptive control system. This makes the stability proof more difficult. Thus, the covariance adjustment for the optimal control modification is different from the standard covariance resetting in least-squares methods.

The covariance adjustment allows for an arbitrary initial adaptive gain to be used. The method then adjusts the adaptive gain toward a lower value to achieve improved robustness while retaining performance. For the standard MRAC, the covariance adjustment generally must be used with the projection method or error modification in order to achieve Lyapunov stability. For systems with matched uncertainty, the optimal control modification eliminates the need for the projection method or error modification and uses the tracking error directly, as can be shown in the

following theorem.

Theorem 1: The optimal control modification with the covariance adjustment is stable and results in ultimate bounds as defined by

$$\|e\| \leq \sqrt{\frac{\lambda_{max}(P)\,\delta^2 + \lambda_{max}(\Gamma^{-1})\,\kappa^2}{\lambda_{min}(P)}} \tag{9}$$

$$\left\|\tilde{\Theta}\right\| \leq \sqrt{\frac{\lambda_{max}(P)\,\delta^2 + \lambda_{max}(\Gamma^{-1})\,\kappa^2}{\lambda_{min}(\Gamma^{-1})}} \tag{10}$$

with $\delta = c_2 + \sqrt{c_2^2 + \frac{\nu c_5 c_6^2}{c_1}}$ and $\kappa = c_6 + \sqrt{c_6^2 + \frac{c_1 c_2^2}{\nu c_5}}$ for $0 \leq \nu < \nu_{max}$ where $c_1 = \lambda_{min}(Q)$, $c_2 = \frac{\lambda_{max}(P) w_0}{\lambda_{min}(Q)}$, $c_5 = \left[\lambda_{min}\left(B^\top A_m^{-\top} Q A_m^{-1} B\right) - \frac{\eta}{\nu}\right]\Phi_0^2$, and $c_6 = \frac{\left\|B^\top P A_m^{-1} B\right\|\Theta_0}{\lambda_{min}\left(B^\top A_m^{-\top} Q A_m^{-1} B\right) - \frac{\eta}{\nu}}$ where $\|\Phi(x)\| \leq \Phi_0$ and $\Theta_0 = \|\Theta^*\|$.

Proof: Using the Lyapunov candidate function

$$V\left(e, \tilde{\Theta}\right) = e^\top P e + \text{trace}\left(\tilde{\Theta}^\top \Gamma^{-1} \tilde{\Theta}\right) \tag{11}$$

and utilizing

$$\frac{d\Gamma^{-1}}{dt} = -\Gamma^{-1}\dot{\Gamma}\Gamma^{-1} = \eta\Phi(x)\Phi^\top(x) \tag{12}$$

then it can be shown that $\dot{V}\left(e, \tilde{\Theta}\right)$ is bounded by

$$\begin{aligned}\dot{V}\left(e, \tilde{\Theta}\right) = -e^\top Q e - 2e^\top P w - \nu\Phi^\top(x)\tilde{\Theta}B^\top A_m^{-\top} Q A_m^{-1} B\tilde{\Theta}^\top\Phi(x) + 2\nu\Phi^\top(x)\Theta^* B^\top P A_m^{-1} B\tilde{\Theta}^\top\Phi(x) \\ + \eta\Phi^\top(x)\tilde{\Theta}\tilde{\Theta}^\top\Phi(x) \leq -c_1\left(\|e(t)\| - c_2\right)^2 - \nu c_5\left(\left\|\tilde{\Theta}\right\| - c_6\right)^2 + c_1 c_2^2 + \nu c_5 c_6^2\end{aligned} \tag{13}$$

for $0 \leq \nu < \nu_{max}$, which implies $0 \leq \eta < \nu\lambda_{min}\left(B^\top A_m^{-\top} Q A_m^{-1} B\right)$.

Thus, $\dot{V}\left(e, \tilde{\Theta}\right) \leq 0$ outside a compact set

$$B_\delta = \left\{\left(e, \tilde{\Theta}\right) \in \mathbb{R}^n \times \mathbb{R}^{m\times p} : c_1\left(\|e\| - c_2\right)^2 + \nu c_5\left(\left\|\tilde{\Theta}\right\| - c_6\right)^2 \leq c_1 c_2^2 + \nu c_5 c_6^2\right\} \tag{14}$$

Therefore, the solution is uniformly ultimately bounded with the ultimate bounds given in Theorem 1.

Corollary 1: If the input function $\Phi(x)$ belongs to a class of functions such that $\|\Phi(x)\| \leq \|x\|$, then

$$\nu_{max} = \frac{\lambda_{min}(P)\,\lambda_{min}(Q)\,\lambda_{min}\left(B^\top A_m^{-\top} Q A_m^{-1} B\right)}{2\lambda_{max}(P)\left\|B^\top P A_m^{-1} B\right\|^2\Theta_0^2}\left[1 + \sqrt{1 - \frac{4\eta\,\lambda_{max}(P)\left\|B^\top P A_m^{-1} B\right\|^2\Theta_0^2}{\lambda_{min}(P)\,\lambda_{min}(Q)\,\lambda_{min}^2\left(B^\top A_m^{-\top} Q A_m^{-1} B\right)}}\right] \tag{15}$$

Proof: ν_{max} is established from the tracking error ultimate bound by letting $\|x\| \to \infty$ in the limit. Then the ultimate

bound can be expressed as

$$\|x_m - x\|^2 \leq \frac{\lambda_{max}(P)}{\lambda_{min}(P)} \left[c_2^2 + \frac{\nu \left\| B^\top P A_m^{-1} B \right\|^2 \Theta_0^2 \|x\|^2}{c_1 \left[\lambda_{min} \left(B^\top A_m^{-\top} Q A_m^{-1} B \right) - \frac{\eta}{\nu} \right]} \right]$$

Therefore, ν_{max} is obtained from

$$1 - \frac{\lambda_{max}(P)\, \nu_{max} \left\| B^\top P A_m^{-1} B \right\|^2 \Theta_0^2}{\lambda_{min}(P)\, \lambda_{min}(Q) \left[\lambda_{min} \left(B^\top A_m^{-\top} Q A_m^{-1} B \right) - \frac{\eta}{\nu_{max}} \right]} = 0 \tag{16}$$

III. Normalized Optimal Control Modification

Normalization is a technique that can be used to achieve more robust adaptation for MRAC. The objective of the normalization is to reduce the effect of the large amplitude of an input function. Normalized adaptation can achieve a significant increase in the time delay margin of a closed-loop adaptive system which indicates robustness. The normalized optimal control modification is expressed as

$$\dot{\Theta} = -\frac{\Gamma}{1 + \Phi^\top(x) R \Phi(x)} \Phi(x) \left[e^\top P - \nu \Phi^\top(x) \Theta B^\top P A_m^{-1} \right] B \tag{17}$$

where $R = R^\top > 0 \in \mathbb{R}^{m \times m}$ is a normalization weighting matrix.

For the standard MRAC, the normalization generally must be used with the projection method or error modification in order to satisfy the Lyapunov stability. Otherwise, proving stability of the normalized standard MRAC can be challenging. To address this difficulty, a number of error modification schemes have been proposed for least-squares adaptive control which uses the estimation error instead of the tracking error. The normalized optimal control modification eliminates the need for the projection method or error modification and uses the tracking error directly for systems with matched uncertainty, as can be shown by the following theorem.

Theorem 2: The normalized optimal control modification (17) is stable and results in a uniform ultimate boundedness of the tracking error for $0 \leq \nu < \nu_{max}$ and normalization weighting matrix $0 \leq R < R_{max}$ such that $\nu c_1 c_3 c_7 - c_8^2 > 0$ where $c_7 = 1 + \lambda_{min}(R)\, \Phi_0^2$ and $c_8 = \|PB\|\, \lambda_{max}(R)\, \Phi_0^3$.

Proof: Using the same Lyapunov candidate function from Theorem 1, then $\dot{V}\left(e, \tilde{\Theta}\right)$ yields

$$\begin{aligned}
\dot{V}\left(e, \tilde{\Theta}\right) = & -e^\top Q e - 2 e^\top P w + \frac{-\nu \Phi^\top(x) \tilde{\Theta} B^\top A_m^{-\top} Q A_m^{-1} B \tilde{\Theta}^\top \Phi(x) + 2\nu \Phi^\top(x) \Theta^* B^\top P A_m^{-1} B \tilde{\Theta}^\top \Phi(x)}{1 + \Phi^\top(x) R \Phi(x)} \\
& + \frac{2 e^\top P B \tilde{\Theta}^\top \Phi(x) \Phi^\top(x) R \Phi(x)}{1 + \Phi^\top(x) R \Phi(x)} \\
\leq & -c_1 \left(\|e\| - c_2 \right)^2 + c_1 c_2^2 + \frac{-\nu c_3 \left(\left\| \tilde{\Theta} \right\| - c_4 \right)^2 + \nu c_3 c_4^2 + 2 \|PB\| \|e\| \left\| \tilde{\Theta} \right\| \lambda_{max}(R) \|\Phi(x)\|^3}{1 + \lambda_{min}(R) \|\Phi(x)\|^2}
\end{aligned} \tag{18}$$

The values of $\|e\|$ and $\left\|\tilde{\Theta}\right\|$ that maximize $\dot{V}\left(e,\tilde{\Theta}\right)$ are evaluated by taking the partial derivatives of $\dot{V}\left(e,\tilde{\Theta}\right)$

$$\frac{\partial \dot{V}\left(e,\tilde{\Theta}\right)}{\partial \|e\|} \leq -2c_1\left(\|e\|-c_2\right)+\frac{2\|PB\|\left\|\tilde{\Theta}\right\|\lambda_{max}(R)\|\Phi(x)\|^3}{1+\lambda_{min}(R)\|\Phi(x)\|^2}=0 \tag{19}$$

$$\frac{\partial \dot{V}\left(e,\tilde{\Theta}\right)}{\partial \left\|\tilde{\Theta}\right\|} \leq \frac{-2\nu c_3\left(\left\|\tilde{\Theta}\right\|-c_4\right)+2\|PB\|\|e\|\lambda_{max}(R)\|\Phi(x)\|^3}{1+\lambda_{min}(R)\|\Phi(x)\|^2}=0 \tag{20}$$

Then $\dot{V}\left(e,\tilde{\Theta}\right)\leq 0$ implies

$$-c_1\left(\|e\|-c_2\right)^2+c_1c_2^2+\frac{c_8^2\|e\|^2}{\nu c_3c_7}+\frac{2c_4c_8\|e\|+\nu c_3c_4^2}{c_7}\leq 0 \tag{21}$$

$$\frac{-\nu c_3\left(\left\|\tilde{\Theta}\right\|-c_4\right)^2+\nu c_3c_4^2+2c_2c_8\left\|\tilde{\Theta}\right\|}{c_7}+c_1c_2^2+\frac{c_8^2\left\|\tilde{\Theta}\right\|^2}{c_1c_7^2}\leq 0 \tag{22}$$

Choose $0\leq R<R_{max}$ and $0<\nu<\nu_{max}$ such that the inequality $\nu c_1c_3c_7-c_8^2>0$ is satisfied. This results in

$$\nu\lambda_{min}(Q)\lambda_{min}\left(B^\top A_m^{-\top}QA_m^{-1}B\right)\Phi_0^2\left[1+\lambda_{min}(R)\Phi_0^2\right]-\|PB\|^2\lambda_{max}^2(R)\Phi_0^6>0 \tag{23}$$

which yields

$$\Phi_0^2<\frac{\nu\lambda_{min}(Q)\lambda_{min}\left(B^\top A_m^{-\top}QA_m^{-1}B\right)\lambda_{min}(R)}{2\|PB\|^2\lambda_{max}^2(R)}\left[1+\sqrt{1+\frac{4\|PB\|^2\lambda_{max}^2(R)}{\nu\lambda_{min}(Q)\lambda_{min}\left(B^\top A_m^{-\top}QA_m^{-1}B\right)\lambda_{min}^2(R)}}\right] \tag{24}$$

Thus, the lower bounds of $\|e\|$ and $\left\|\tilde{\Theta}\right\|$ are established as

$$\|e\|\geq\delta=\frac{\nu c_3\left(c_1c_2c_7+c_4c_8\right)}{\nu c_1c_3c_7-c_8^2}\left[1+\sqrt{1+\frac{c_4^2\left(\nu c_1c_3c_7-c_8^2\right)}{\left(c_1c_2c_7+c_4c_8\right)^2}}\right] \tag{25}$$

$$\left\|\tilde{\Theta}\right\|\geq\kappa=\frac{c_1c_7\left(\nu c_3c_4+c_2c_8\right)}{\nu c_1c_3c_7-c_8^2}\left[1+\sqrt{1+\frac{c_2^2\left(\nu c_1c_3c_7-c_8^2\right)}{\left(\nu c_3c_4+c_2c_8\right)^2}}\right] \tag{26}$$

Therefore, $\dot{V}\left(e,\tilde{\Theta}\right)\leq 0$ outside a compact set

$$B_\delta=\left\{\left(e,\tilde{\Theta}\right)\in\mathbb{R}^n\times\mathbb{R}^{m\times p}:c_1\left(\|e\|-c_2\right)^2+\frac{\nu c_3\left(\left\|\tilde{\Theta}\right\|-c_4\right)^2-2c_8\|e\|\left\|\tilde{\Theta}\right\|}{c_7}\leq c_1c_2^2+\frac{\nu c_3c_4^2}{c_7}\right\} \tag{27}$$

The closed-loop system is uniformly ultimately bounded for $0<\nu<\nu_{max}$ and $0\leq R<R_{max}$.

IV. Flight Experiments

Flight experiments of three adaptive controllers was conducted from November 2010 to January 2011 onboard the NASA Full-scale Advanced Systems Testbed (FAST), which is an F/A-18 aircraft, tail number 853.[27,28] The first adaptive controller is a simple MRAC. The second and third adaptive controllers are based on the normalized optimal control modification. The avionics include an ARTS (Airborne Research Test System) flight control computer system. Failure emulations were introduced via parameter changes in the flight control software to intentionally degrade aircraft stability and through hardware emulated faults by means of frozen stabilator and cross-coupled pilot stick inputs.[27,28] The flight test results indicate that the three adaptive controllers were able to restore performance of the F/A-18 aircraft in most cases, and the optimal control modification was noted to perform quite well and adapt more quickly than the simple MRAC for the reduced pitch damping failure.

In 2009, a request for information (RFI) was released by the NASA Integrated Resilient Aircraft Control (IRAC) project seeking ideas for adaptive control flight experiments. One of the focus areas identified from the responses that NASA received was to investigate simple yet effective adaptive control algorithms to help address the issue of verification and validation (V&V) testing of adaptive control. Adaptive controllers, such as the standard MRAC, face many difficulties with regards to certification for commercial or military aircraft. There are large gaps in the certification process for dealing with adaptive controllers.[20,21] Adaptive controllers can become complex with many adaptive parameters and complex update laws as well as nonlinearity. The required V&V testing can require extensive and exhaustive Monte-Carlo testing. By simplifying an adaptive controller, the required testing could potentially be greatly reduced. Simplification is often at the expense of performance and the controller's ability to handle more complex failure conditions. So, there exists a trade-off between complexity and performance.

Previous flight experiments of neural network adaptive control conducted by the NASA Intelligent Flight Control System (IFCS) project on a NASA NF-15B aircraft, tail number 837 from 2002 to 2006 offer valuable lessons learned regarding the complexity of adaptive control.[22] The IFCS was based on the *e*-modification with sigma-pi neural network originally developed by Calise.[23] During the first phase, Gen-IIa, the sigma-pi network utilized a large input set. The flight test in 2004 showed that the IFCS did not perform as well as it did in simulations. In some instances, the IFCS generated large commands that caused load limit excursions. A subsequent modification in the second phase, Gen-IIb, to simplify the sigma-pi network with a much simplified input set demonstrated an improvement of the IFCS in simulations. However, during the flight test in 2006, mixed results were obtained. Lateral pilot-induced oscillations (PIOs) were experienced for an in-flight simulated stabilator failure. A study was conducted at the end of the IFCS project and showed that the normalization performed better than the Gen-IIb IFCS in simulations.

A. Flight Simulator Pilot Study

Based on the RFI and the lessons learned from the IFCS flight experiment, a decision was made to conduct follow-on flight experiments. The process of selecting which adaptive control should be flown involved reviewing the literature and simulation results from high-fidelity flight simulations. During 2009, NASA Ames Research Center conducted an extensive pilot evaluation of several adaptive controllers in a motion-based flight simulator, the Advanced Concepts Flight Simulator (ACFS).[24,25] The ACFS employs an advanced digital fly-by-wire flight control system. A high-fidelity flight dynamic model of a NASA GTM (Generic Transport Model) was implemented with failure and damage emulations including asymmetric damage to the left horizontal tail and elevator, flight control faults emulated by scaling the B-matrix, and combined failures. Eight different NASA test pilots participated in the study. Seven adaptive controllers were evaluated, namely; e-modification (MRAC),[3] optimal control modification (OCM),[9] adaptive loop transfer recovery (ALR),[5] composite or predictor-based MRAC (PMRAC),[8] $\mathscr{L}_1$ adaptive control,[4] hybrid adaptive control,[26] and bounded linear stability metric-driven adaptive control (BLS).[29,30] Each pilot performed a series of tasks and provided Cooper-Harper (CH) ratings for those tasks, which included large amplitude attitude capture and cross-wind approach and landing.

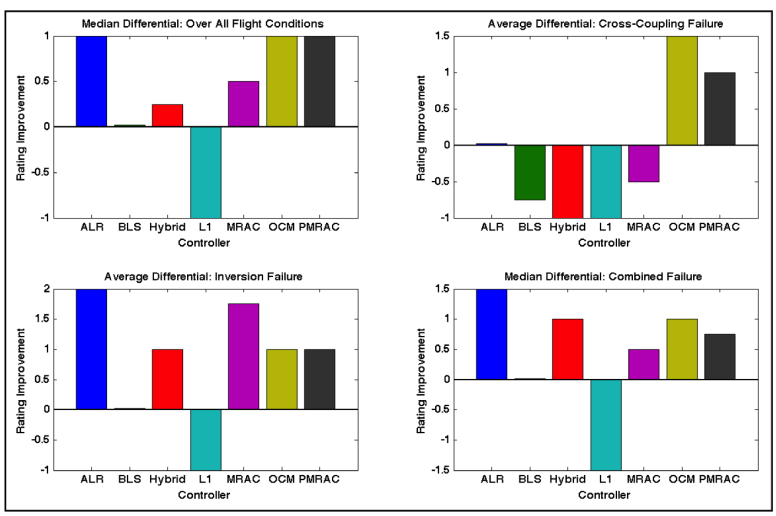

Figure 1. Cooper-Harper Ratings Differentials (Positive Value Indicates Improved Performance)

Figure 1 shows the relative improvements in the CH ratings of the seven adaptive controllers over the baseline controller for all different failure emulations.[25] The study confirms that adaptive control can clearly provide significant benefits by improving flight control performance in adverse conditions. The study also provides an insight into the role of pilot interactions with adaptive control. It was observed that many favorable pilot ratings were associated with those adaptive controllers that tended to be predictable. In general, the optimal control modification performed well over all flight conditions as compared to the e-modification. In particular, the optimal control modification outperformed the

e-modification in all cases but the dynamic inversion failure. Furthermore, the cross-coupling failure presented itself as a particular challenge to several adaptive controllers, only two of which including the optimal control modification were able to demonstrate improvement.

B. F/A-18 Flight Simulations

A further investigation of the optimal control modification was performed for a high-fidelity F/A-18 aircraft model.[19] The flight condition is a test point of Mach 0.5 at 15,000 ft. All of the pilot inputs to the simulation time histories are from "canned" piloted stick inputs and no attempts to correct for the aircraft attitudes are added to the piloted inputs. This "canned pilot input" method is used only for comparison purposes. For instance, when a failure is imparted on the aircraft and the resulting attitude changes minimally, the control system is said to have good restoring properties. All the test cases have a one-frame delay (1/100 sec) at the actuators for added realistic implementation purposes.

The first case is an A-matrix failure with a destabilizing center of gravity (CG) shift or a C_{m_α} change. Figure 2 shows a 40-sec time history in which three longitudinal pilot stick inputs are presented and the failure is imposed at 13 sec. In the first 13 sec, a normal health response shows how the pitch rate follows the commanded pitch rate (green). After the failure is inserted, the response without adaptation shows that the aircraft is stable but with low damping and two overshoots (blue). With adaptation on (red), the response is much better and follows the commanded pitch rate. Figure 2 also shows the angle of attack and normal acceleration responses and that the system behaves better with adaptation than without. Figure 3 shows the tracking errors in the roll, pitch and yaw axes along with the adaptation weights. The results show that the adaptation helps the pitch tracking task and increases the damping.

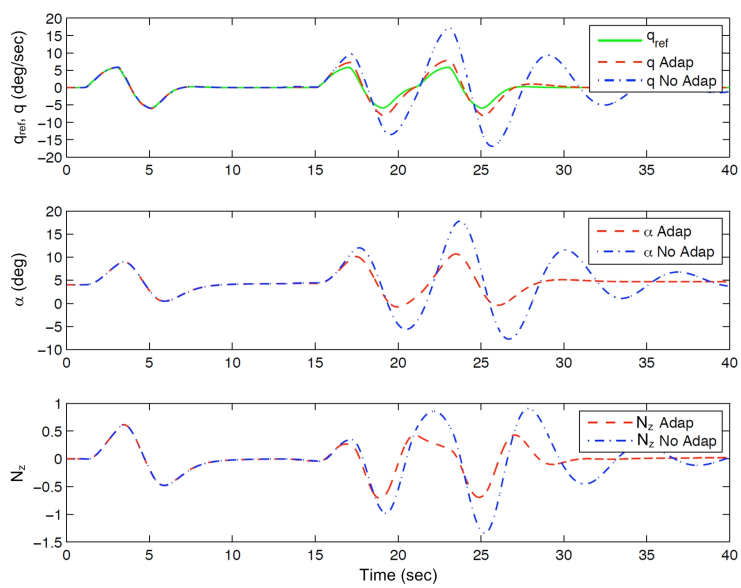

Figure 2. Longitudinal Response due to an $A-$Matrix Failure (C_{m_α} Shift at 13 sec)

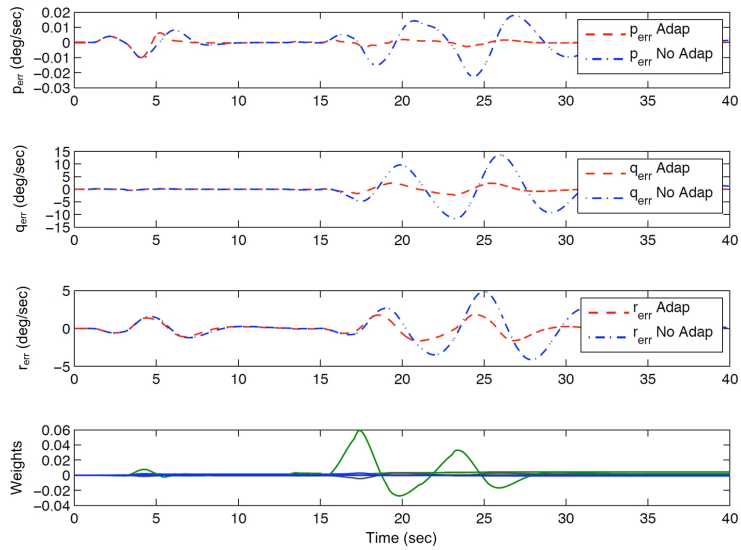

Figure 3. Tracking Errors and Weights due to an $A-$Matrix Failure (C_{m_α} Shift at 13 sec)

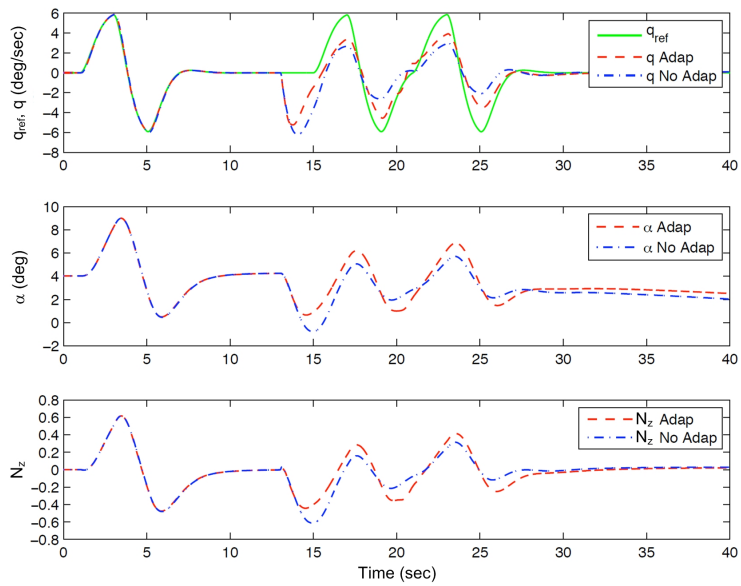

Figure 4. Longitudinal Response due to a B-Matrix Failure (Stabilator Jammed at 2.5^{o}at 13 sec)

The second case is a B-matrix failure imposed on the left stabilator at 13 sec. The left stabilator is jammed at +2.5° from trim. Figure 4 shows a 40-sec time history of the longitudinal responses. During the first 13 sec, the pitch rate follows the commanded pitch rate, but after the failure insertion there is a large downward motion and the system cannot track well without adaptation. Pitch rate follows the reference signal better with adaptation on. The lateral-directional responses from the same longitudinal command also show better aircraft response with adaptation, as shown in Fig. 5. The roll rate with adaptation is smaller than without adaptation. The bank angle and sideslip angle both decrease with adaptation but stay at 10° and 8°, respectively, without adaptation. Figure 6 shows smaller tracking

errors and converging adaptation weights.

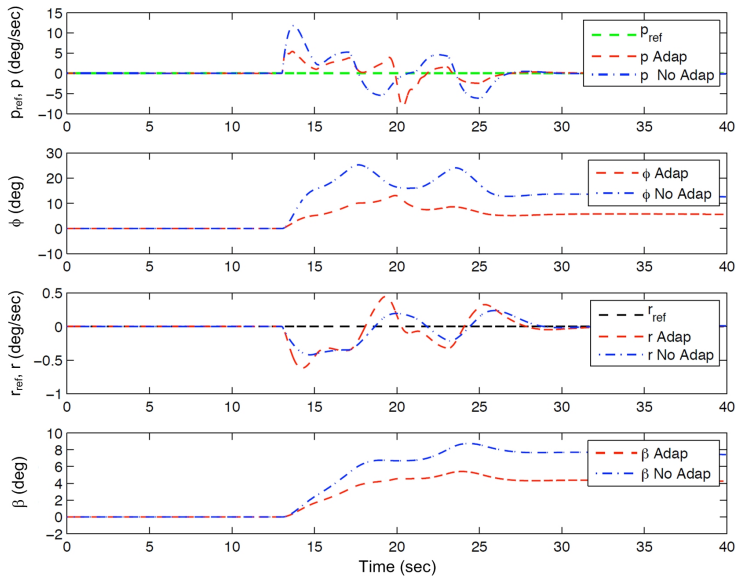

Figure 5. Lateral-Directional Response due to a *B*-Matrix Failure (Stabilator Jammed at 2.5^o at 13 sec)

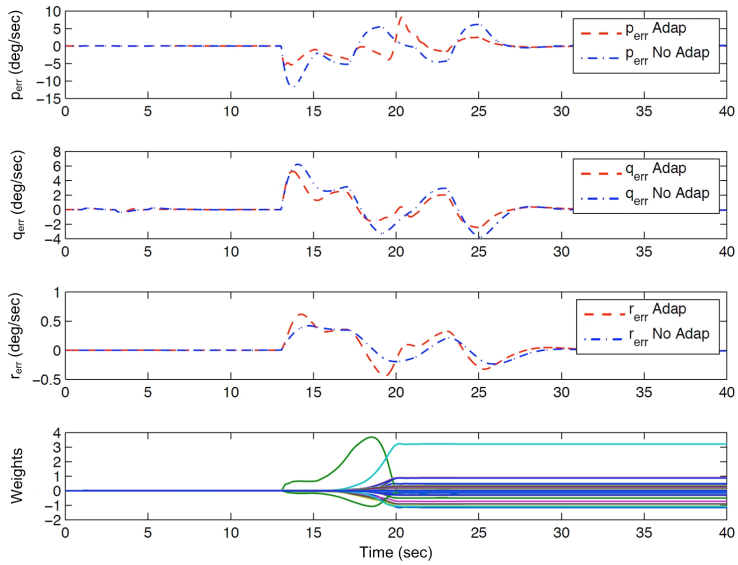

Figure 6. Tracking Errors and Weights due to a *B*-Matrix Failure (Stabilator Jammed at 2.5^o at 13 sec)

Simulations are also conducted to show that the adaptive gain can be increased and the aircraft will remain stable. The test case changes the adaptation rate from 0.5 to 50 while keeping the modification parameter ν constant at 1. Figure 7 shows the same *A*-matrix failure occurring at 2 sec instead of at 13 sec and is followed by a pitch input. As Fig. 7 shows, the pitch rate tracking error is large with an adaptive gain Γ of 0.5 compared to 50. The weights are also shown, and the larger adaptive gain increases the size of the weights. The weights are convergent and the tracking error is better with the larger adaptive gain. Figure 8 shows the response when ν is changed from 0.25 to 1 while

keeping the adaptive gain constant at $\Gamma = 5$. The tracking error has low damping with the lower value of $\nu = 0.25$ as expected. In both cases the weights converge to reasonable values. The results show that larger adaptive gains can be tolerated with the optimal control modification.

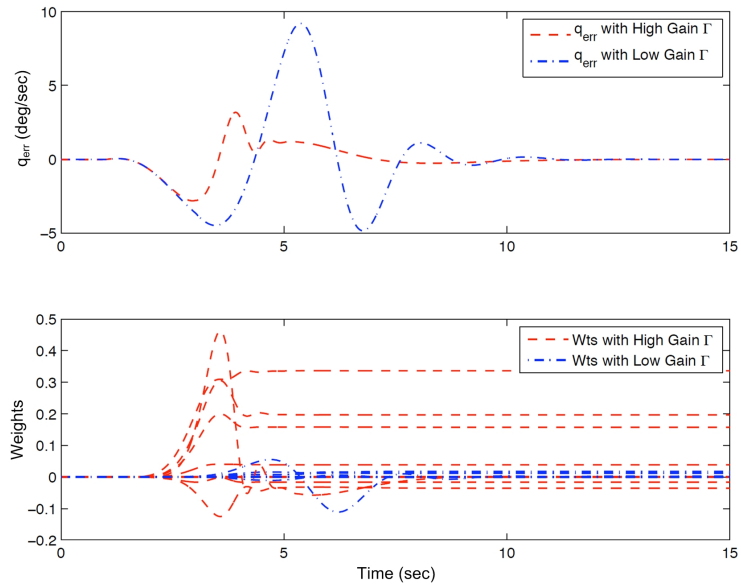

Figure 7. Pitch Rate Error and Weights due to an A-Matrix Failure (C_{m_α} Shift at 2 sec) for $\Gamma = 0.5$ and $\Gamma = 50$ with Fixed $\nu = 1$

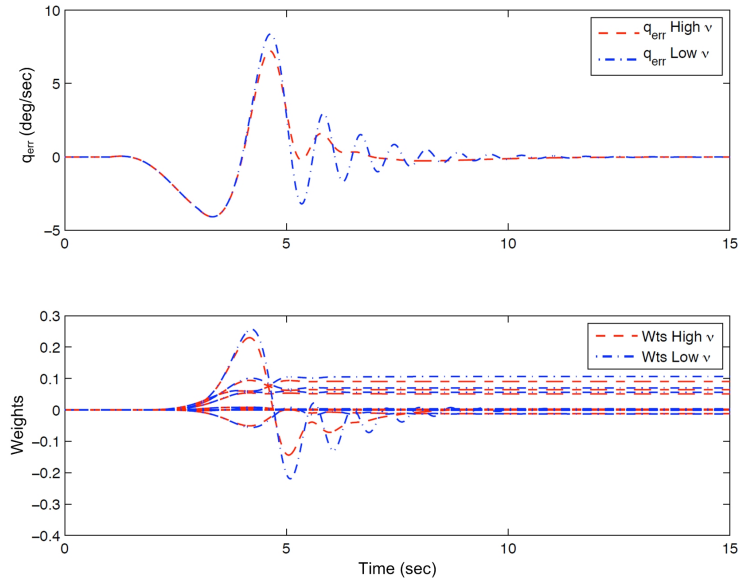

Figure 8. Pitch Rate Error and Weights due to an A-Matrix Failure (C_{m_α} Shift at 2 sec) for Fixed $\Gamma = 5$ with $\nu = 0.25$ and $\nu = 1$

C. Adaptive Flight Control Architecture for FAST

Figure 9 shows the nonlinear dynamic inversion (NDI) control architecture implemented on the NASA FAST aircraft.[27] The NDI controller is augmented by an adaptive controller that includes a simple MRAC, and the normalized optimal

control modification with and without adaptive disturbance estimation. The optimal control modification is considered as a more complex MRAC for evaluating the trade-off between complexity and performance in the flight experiments.

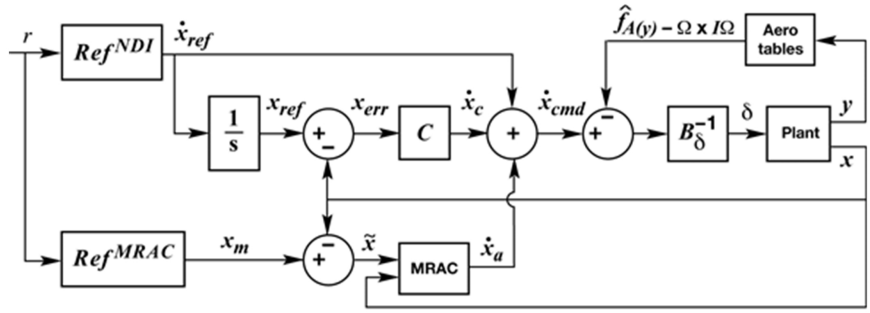

Figure 9. Nonlinear Dynamic Inversion Adaptive Flight Control System

The control input vector δ has ten control surface commands and is computed by the NDI controller as

$$\delta = B_{\delta}^{-1}\left[I\dot{x}_{cmd} + \Omega \times I\Omega - \hat{f}_A(y)\right] + \delta_0 \tag{28}$$

where the vector of estimated aerodynamic moments $\hat{f}_A(y)$ is calculated from onboard aerodynamic lookup tables, while the angular rates Ω are measured using aircraft sensors, I is the inertia matrix of the aircraft, δ_0 are pre-determined trim surface commands, and B_{δ}^{-1} is a weighted pseudo-inverse of the control sensitivity matrix weighted by a control allocation matrix computed as

$$B_{\delta}^{-1} = W^{-1}B_{\delta}^{\top}\left(B_{\delta}W^{-1}B_{\delta}^{\top}\right)^{-1} \tag{29}$$

The angular acceleration commands $\dot{x}_{cmd}(t)$ contain the sum of the desired reference dynamics $\dot{x}_{ref}(t)$ produced by the NDI reference model, the output $\dot{x}_c(t)$ of the error compensator, and the adaptive augmentation $\dot{x}_a(t)$ computed by the adaptive controller, which only provides the augmentation in the pitch and roll axes.

$$\dot{x}_{cmd} = \dot{x}_{ref} + \dot{x}_c + \dot{x}_a = \begin{bmatrix} \dot{p}_{ref} + \dot{p}_c + \dot{p}_a \\ \dot{q}_{ref} + \dot{q}_c + \dot{q}_a \\ \dot{r}_{ref} + \dot{r}_c \end{bmatrix} \tag{30}$$

The NDI reference model is specified by the pilot command $r(t)$ in the pitch and roll axes and generally represents the same desired dynamics as the adaptive control reference model. It may also be modified to emulate a failure or damaged plant dynamics. The state feedback vector $y(t)$ contains measurements of the inputs required for the aerodynamic lookup tables, such as angle of attack and velocity, as well as the angular rates.

The adaptive control reference model is specified as a stable, linear time-invariant system as

$$\dot{x}_m = \begin{bmatrix} \dot{p}_m \\ q_m \\ \dot{q}_m \end{bmatrix} = \begin{bmatrix} -\omega_p & 1 & 0 \\ 0 & 0 & 1 \\ 0 & -\omega_q^2 & -2\zeta_q\omega_q \end{bmatrix} \begin{bmatrix} p_m \\ \int_0^t q_m(\tau)\,d\tau \\ q_m \end{bmatrix} + \begin{bmatrix} 1 & 0 \\ 0 & 0 \\ 0 & 1 \end{bmatrix} \begin{bmatrix} r_p \\ r_q \end{bmatrix} \tag{31}$$

The pitch axis reference model is second-order, representing the desired short-period dynamics specified by the reference model frequency ω_q and damping ratio ζ_q. The roll axis reference model is first-order specified by the eigenvalue ω_p. There is no yaw axis reference model, but a second-order model could be used to represent the desired dutch-roll dynamics, if needed.

The pilot commands $r_p(t)$ and $r_q(t)$ are computed from the pilot stick inputs $\delta_{lat}(t)$ and $\delta_{lon}(t)$ according to

$$\begin{bmatrix} r_p \\ r_q \end{bmatrix} = \begin{bmatrix} \left(\frac{r_{max}}{\alpha}\right) k_p \omega_p \delta_{lat} \\ k_q \omega_q^2 \left[\delta_{lon} + L_a \int_0^t \delta_{lon}(\tau)\,d\tau\right] \end{bmatrix} \tag{32}$$

The error compensator is necessary to improve tracking of the reference model in the presence of model uncertainty and disturbances by the NDI controller without adaptive augmentation. The NDI controller contains a proportional-integral error compensator in the pitch axis and a proportional error compensator in the roll axis. The gains of the error compensator are tuned to match the reference model. Thus

$$\begin{bmatrix} \dot{p}_c \\ \dot{q}_c \end{bmatrix} = \begin{bmatrix} \omega_p\left(p_{ref} - p\right) \\ 2\zeta_q\omega_q\left(q_{ref} - q\right) + \omega_q^2 \int_0^t \left[q_{ref}(\tau) - q(\tau)\right] d\tau \end{bmatrix} \tag{33}$$

The aircraft true, unknown dynamics are written as

$$\dot{x} = \begin{bmatrix} \dot{p} \\ q \\ \dot{q} \end{bmatrix} = \begin{bmatrix} -(\omega_p + \theta_p) & 1 & 0 \\ 0 & 0 & 1 \\ 0 & -\left(\omega_p^2 + \theta_{q_1}\right) & -(2\zeta_p\omega_p + \theta_{q_2}) \end{bmatrix} \begin{bmatrix} p \\ \int_0^t q(\tau)\,d\tau \\ q \end{bmatrix} + \begin{bmatrix} 1 & 0 \\ 0 & 0 \\ 0 & 1 \end{bmatrix} \begin{bmatrix} u_p - \sigma_p \\ u_q - \sigma_q \end{bmatrix} \tag{34}$$

where θ_p, θ_{q_1}, and θ_{q_2} are unknown but constant parameters, and $\sigma_p(t)$ and $\sigma_q(t)$ are scalar, time-varying uncertain disturbances.

The NDI adaptive controller is designed to cancel out the effects of the uncertain parameters θ_p, θ_{q_1}, θ_{q_2}, $\sigma_p(t)$, and $\sigma_q(t)$ by the adaptive augmentation. This is expressed as

$$\begin{bmatrix} u_p \\ u_q \end{bmatrix} = \begin{bmatrix} r_p + \dot{p}_a \\ r_q + \dot{q}_a \end{bmatrix} = \begin{bmatrix} r_p + \hat{\theta}_p p + \hat{\sigma}_p \\ r_q + \hat{\theta}_{q_1} \int_0^t q(\tau)\,d\tau + \hat{\theta}_{q_2} q + \hat{\sigma}_q \end{bmatrix} \tag{35}$$

Three adaptive controllers were implemented. They are: 1) simple MRAC, 2) normalized optimal control modification, and 3) normalized optimal control modification plus adaptive disturbance estimation. These adaptive controllers vary in complexity from the simplest to a more complex design.

1. The simple MRAC controller, designated as "sMRAC", employs only a single-axis input in either the roll or pitch axis. The sMRAC laws are used to estimate the uncertain parameters θ_p, θ_{q_1} and θ_{q_2} as

$$\dot{\hat{\theta}}_p = \Gamma_{\theta_p} p \tilde{p} P_p B_{m_p} \tag{36}$$

$$\dot{\hat{\theta}}_q = \Gamma_{\theta_q} x_q \tilde{x}_q^\top P_q B_{m_q} \tag{37}$$

where $\hat{\theta}_q = \begin{bmatrix} \hat{\theta}_{q_1} & \hat{\theta}_{q_2} \end{bmatrix}^\top$, $\tilde{p} = p_m - p$, $x_q = \begin{bmatrix} \int_0^t q(\tau)\, d\tau & q \end{bmatrix}^\top$, and $\tilde{x}_p = \begin{bmatrix} \int_0^t [q_m(\tau) - q(\tau)]\, d\tau & q_m - q \end{bmatrix}^\top$.

2. The normalized optimal control modification, designated as "onMRAC", represents a more complex design. The onMRAC laws are described by

$$\dot{\hat{\theta}}_p = \frac{\Gamma_{\theta_p}}{1 + N_{\theta_p} p^2} \left(p \tilde{p} P_p B_{m_p} + \nu_{\theta_p} p^2 \hat{\theta}_p B_{m_p}^\top P_p A_{m_p}^{-1} B_{m_p} \right) \tag{38}$$

$$\dot{\hat{\theta}}_q = \frac{\Gamma_{\theta_q}}{1 + x_q^\top N_{\theta_q} x_p} \left(x_q \tilde{x}_q^\top P_q B_{m_q} + \nu_{\theta_q} x_q x_q^\top \hat{\theta}_q B_{m_q}^\top P_q A_{m_q}^{-1} B_{m_q} \right) \tag{39}$$

where N_{θ_p} and N_{θ_q} are the weighting parameters for the normalization factors and ν_{θ_p} and ν_{θ_q} are the modification parameters.

3. The effect of disturbances can also be accounted for in the adaptive controller by employing adaptive laws for disturbance estimation to cancel out the effects of the disturbances $\sigma(t)$. This adaptive controller is referred to as "onMRAC+" which includes the following adaptive laws in addition to the onMRAC:

$$\dot{\hat{\sigma}}_p = \frac{\Gamma_{\sigma_p}}{1 + N_{\sigma_p} p^2} \left(\tilde{p} P_p B_{m_p} + \nu_{\sigma_p} \hat{\sigma}_p B_{m_p}^\top P_p A_{m_p}^{-1} B_{m_p} \right) \tag{40}$$

$$\dot{\hat{\sigma}}_q = \frac{\Gamma_{\sigma_q}}{1 + x_q^\top N_{\sigma_p} x_p} \left(\tilde{x}_q^\top P_q B_{m_q} + \nu_{\sigma_q} \hat{\sigma}_q B_{m_q}^\top P_q A_{m_q}^{-1} B_{m_q} \right) \tag{41}$$

The onMRAC+ is the most complex design in the flight experiments. The disturbance estimation adaptive law in the pitch axis was implemented without the optimal control modification term by setting $\nu_{\sigma_q} = 0$ to aid in the investigation of the usefulness of the optimal control modification term. The inclusion of the normalization without the optimal control modification term in the pitch axis contrasts with the inclusion of both terms in the roll axis and provides insight into whether the normalization alone is sufficient to ensure desirable adaptive

parameter characteristics. During the post-flight test data analysis, it appeared that this term would have been able to further improve the performance in the pitch axis.

D. Flight Test Results

The failures were emulated during the flight experiments as changes in the pitch and roll damping derivatives to intentionally degrade the pitch and roll handling qualities. Undesired pitch-roll coupling was also emulated in the flight experiments by a roll-to-pitch input coupling and a frozen left stabilator. The flight controllers were tuned for a single flight condition of Mach 0.58 and 25,000 ft. This airspeed-altitude combination falls within the envelope cleared for the FAST aircraft in which any unexpected control surface deflection combination will not exceed structural load limits and ensures that there is adequate altitude for recovery in the case of a departure from controlled flight.

Initial evaluations of the baseline NDI controller and the three adaptive controllers were completed for a healthy aircraft as well as for an 80% reduction in the pitch damping derivative C_{m_q} and a 117% reduction in the roll damping derivative C_{l_p}, resulting in a sign reversal. The reduced pitch and roll damping failures were implemented by altering the values of C_{m_q} and C_{l_p} in the aerodynamic lookup tables.

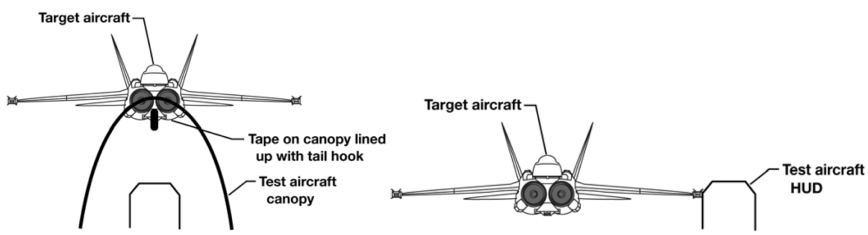

Figure 10. Gross Acquisition Starting Point and Gross Acquisition Ending Point and Fine Tracking Reference Point

A set of tasks was developed for handling quality evaluation that incorporated coupling in both the pitch and roll axes. The setup for the tasks involved having the test aircraft fly in-trail behind a target aircraft. A piece of tape was placed on the canopy of the test aircraft and aligned with the tail hook of the target aircraft as a marker, as shown in Fig. 10. The horizontal spacing was set at two ship lengths (one ship length is 56 ft).[27] Once in this position, the pilot selected the failure on the flight computer by pressing the nose wheel steering button. The pilot then began the first task which is a gross acquisition task, where the pilot of the test aircraft maneuvered the plane to line up a reference point on the heads-up display (HUD) with the wingtip of the target aircraft while maintaining the two-ship length spacing, as shown in Fig. 10. The task was repeated by going to both sides because the failures were asymmetric so an assessment in both directions was necessary. Following gross acquisition, the pilot initiated the fine tracking task by holding the HUD reference point on to the wingtip for at least 10 to 15 sec.[27]

Two pilots flew the handling qualities tasks for the reduced pitch and roll damping. Handling qualities ratings given by Pilot A and Pilot B during a 2-g air-to-air tracking task with the reduced pitch damping failure are shown

in Fig. 11.[28] Due to the high workload required to maintain pitch control in gross acquisition, Pilot B was unable to maintain sufficient airspeed to complete the fine tracking portion of the task with the baseline NDI controller, and consequently no rating was given for that case. An overall assessment of the ratings indicate that all the adaptive controllers improved the handling qualities during the gross acquisition task, but that the varying levels of controller complexity had some effect on the CH ratings for Pilot A but not Pilot B. The CH ratings for Pilot A show that the onMRAC and onMRAC+ performed better than the sMRAC. In all cases, the baseline NDI controller performed worse than the adaptive controllers. For the fine tracking task, both Pilot A and Pilot B reported little to no improvement in the CH ratings for the sMRAC and onMRAC, while Pilot A noted some improvement with the onMRAC+.

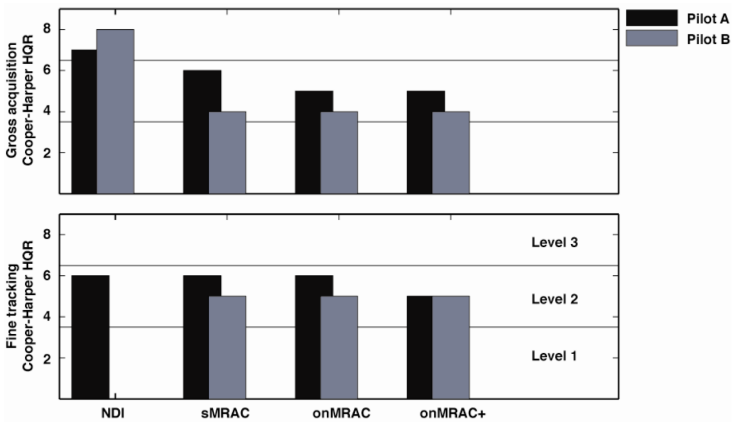

Figure 11. Handling Qualities Ratings for 2-g Tracking Task with Reduced Pitch Damping Failure

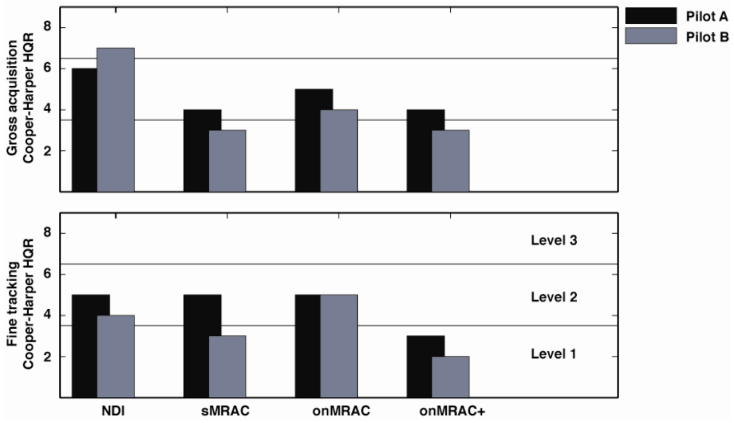

Figure 12. Handling Qualities Ratings for Formation Tracking Task with Reduced Roll Damping Failure

The CH ratings of Pilot A and Pilot B for gross acquisition and fine tracking with the reduced roll damping failure are shown in Fig. 12.[28] Both pilots rated the baseline NDI controller with no failures (not shown) as Level 1 for this task, with Pilot A giving it CH ratings of 2 and 3, and Pilot B giving it ratings of 3 for gross acquisition and 2 for fine tracking. The failure degraded the gross acquisition handling qualities more than those for the fine tracking task. All

the adaptive controllers improved the gross acquisition ratings, but the fine tracking results were less conclusive. The onMRAC+ performed as well or better than the sMRAC and onMRAC, completely restoring the Level 1 fine tracking handling qualities of the baseline NDI controller with no failures.

Three pilots flew the handling qualities tasks with the roll-to-pitch input coupling failure. Figure 13 shows both the CH and PIO ratings for the gross acquisition task.[27] For the CH ratings, every pilot gave Level 2 handling qualities for the baseline NDI controller with the failure. With the adaptive controllers on, handling qualities either remained at Level 2 or improved to Level 1 for all pilots. Pilot A and Pilot C showed similar trends. They both gave PIO ratings of 1 for all the controllers, which indicate that no undesirable motion was noticed even though coupling between the axes was present. Based on the CH ratings, the workload for the task was reduced with the sMRAC and onMRAC+, and the onMRAC showed either equal or improved workload from that of the baseline NDI controller with the failure. The ratings indicated that both pilots A and C were not too sensitive to the roll-to-pitch input coupling failure.

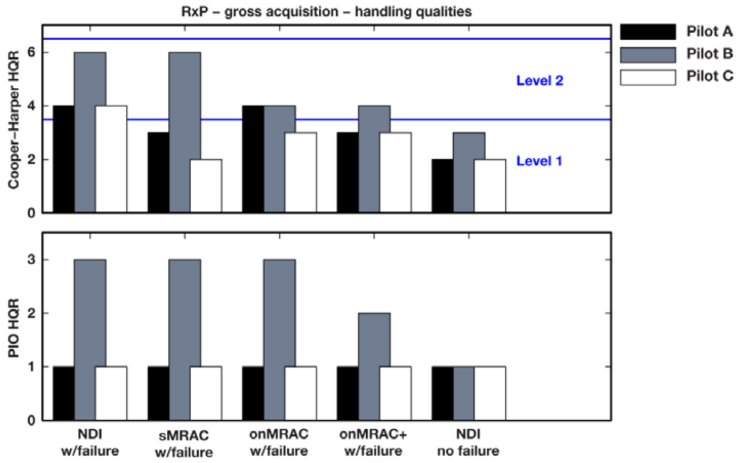

Figure 13. Handling Qualities Ratings for Gross Acquisition with Roll-to-Pitch Input Coupling Failure

On the other hand, pilot B was much more sensitive to the failure because he rated the failure as having undesirable motion that affected his ability to perform the task and specifically mentioned that he felt coupling. Pilot B also gave the worst CH rating of 6 for the baseline NDI controller. With the sMRAC, he was still getting just adequate performance with the same level of workload. With the onMRAC, however, he saw improvement and was able to get desired performance, but the undesirable motion was still a factor. With the onMRAC+, this was no longer the case and he gave a PIO rating of 2, meaning the task performance was no longer compromised by the failure. For onMRAC+, his CH and PIO ratings showed considerable improvement in reducing the effect of the failure.

Figure 14 shows the magnitude of coupling of pitch rate due to roll rate.[27] The magnitude of coupling was calculated based on the ADS-33E standard for cross-coupling handling qualities criteria for helicopters[31] and similar criteria for fixed-wing aircraft developed by the U.S. Air Force Test Pilot School using an F-16 aircraft for the project Icarus.[32] The value was averaged over this task as the adaptation occurred. For each pilot, the magnitude of coupling

was seen to generally decrease as controller complexity was added to the adaptation, thereby illustrating the trade-off between performance and complexity. Thus, the onMRAC+ was able to reduce the effect of the roll-to-pitch coupling failure better than sMRAC even though it is the most complex adaptive controller.

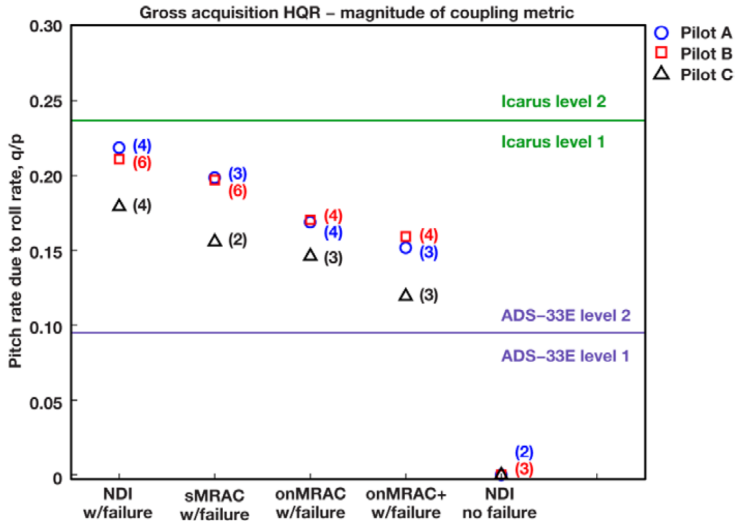

Figure 14. Magnitude of Coupling for Gross Acquisition with Roll-to-Pitch Input Coupling Failure

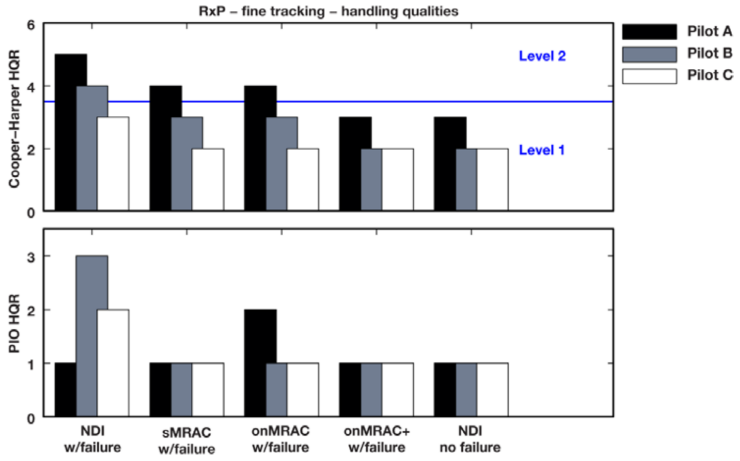

Figure 15. Handling Qualities Ratings for Fine Tracking with Roll-to-Pitch Input Coupling Failure

Figure 15 shows the handling qualities ratings for the fine tracking task.[27] The onMRAC+ with the failure received the same CH and PIO ratings as the baseline NDI controller with no failures. Thus, the onMRAC+ had effectively removed the failure. For all pilots, as controller complexity was added, the CH ratings either stayed the same or improved. Based on the PIO scale, no pilot saw any PIOs; however, undesirable motions were observed. The most undesirable motion was observed for the baseline NDI controller with the failure by both Pilot B and Pilot C.

Figure 16 shows that the magnitude of coupling was reduced as controller complexity was added.[27] There appears to be a correlation between the amount of coupling the pilots experienced and the CH ratings given, with both showing

improvement with added controller complexity.

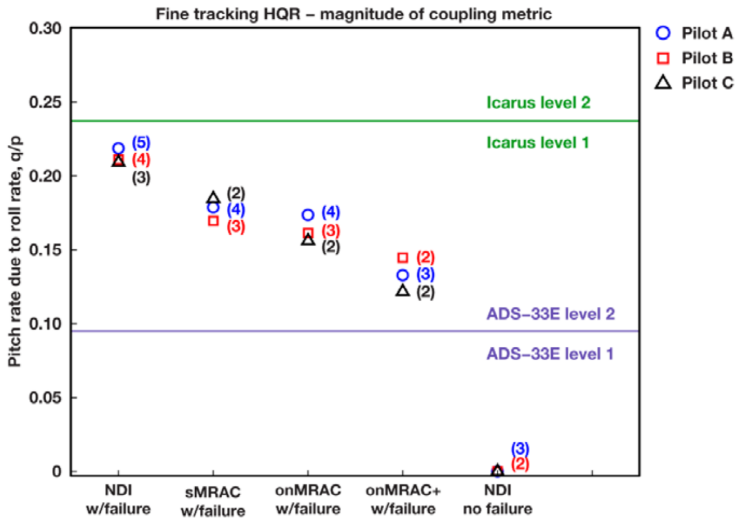

Figure 16. Magnitude of Coupling for Fine Tracking with Roll-to-Pitch Input Coupling Failure

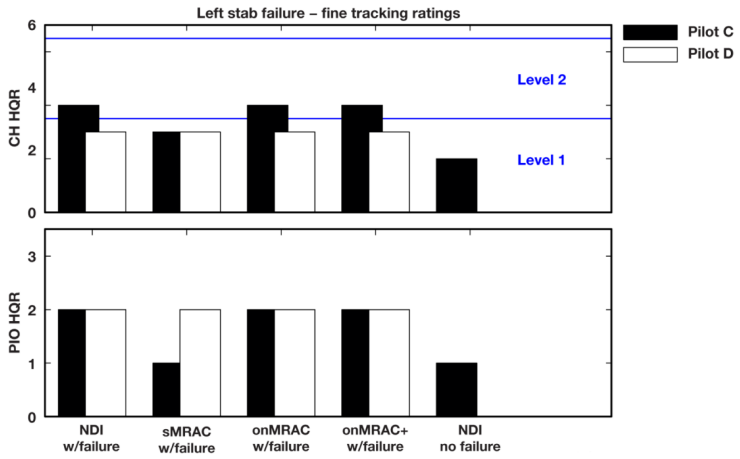

Figure 17. Handling Qualities Ratings for Fine Tracking with Frozen Left Stabilator Failure

Two pilots flew the handling qualities tasks with the left stabilator frozen at zero deflection, a slight offset from trim. For the gross acquisition task, both pilots rated the failure with the NDI and the three adaptive controllers within Level 2 showing no improvement, as shown in Fig. 17.[27] Pilot D gave all the controllers the same CH and PIO ratings. Pilot C observed some improvement with the sMRAC in both CH and PIO ratings, and no improvement with the onMRAC and onMRAC+.

Figures 18 and 19 show the tracking error measure, which is computed as the square root of the integral of the tracking error square, produced by Pilot C in the roll and pitch axes, respectively.[27] The NDI controller produced the largest roll tracking error. All three adaptive controllers were able to reduce the roll tracking error substantially, but the onMRAC+ had a larger roll tracking error than either the sMRAC or onMRAC. In the pitch axis, the tracking error

was greatest with the onMRAC. The sMRAC had a similar pitch tracking error as the NDI controller. The onMRAC+ performed the best with a substantially lower pitch tracking error than any other controllers. The pitch tracking error issue with the onMRAC was traced back to the response of the $\hat{\theta}_{q_2}$ term, which was seen to increase more rapidly than with the sMRAC or onMRAC+ and exhibited an oscillatory behavior. This was seen as a contributing factor to the lower ratings by Pilot C. On the other hand, the onMRAC+ had similar ratings as the onMRAC even though the onMRAC+ reduced the tracking error substantially in both axes. Simulation tests conducted after the flight experiments showed that these issues can be greatly reduced by changing the normalization method and with further tuning.[27]

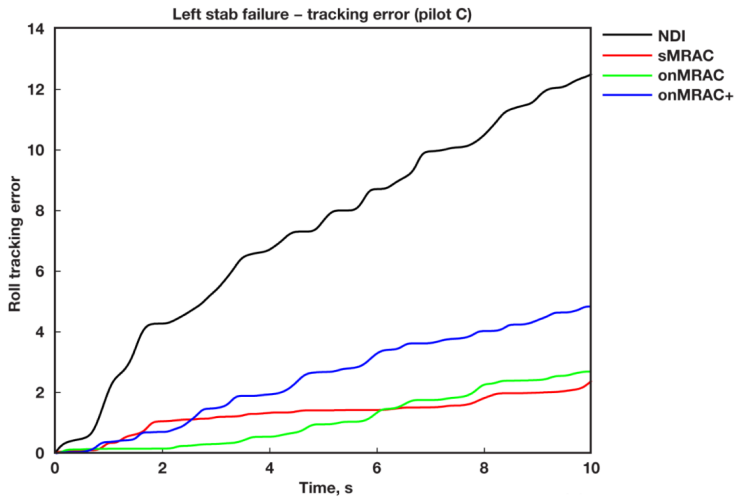

Figure 18. Roll Tracking Error for Fine Tracking with Frozen Left Stabilator Failure

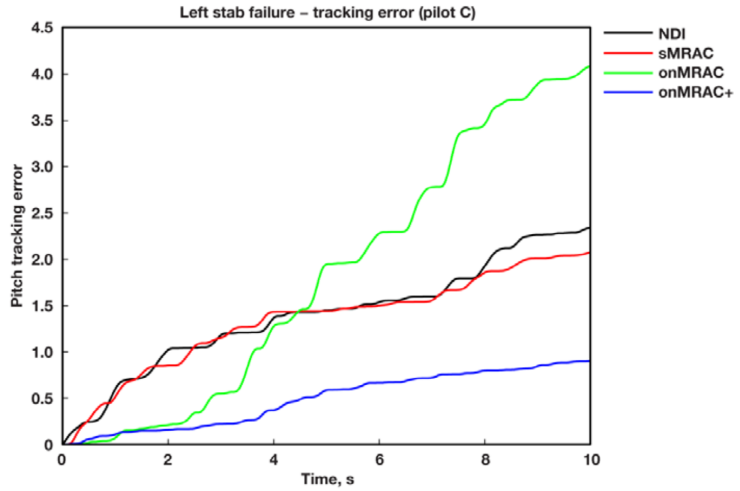

Figure 19. Pitch Tracking Error for Fine Tracking with Frozen Left Stabilator Failure

It was found that the normalization suppresses adaptation during large dynamic maneuvers through attenuation of the adaptive gain by the inverse of the weighted square of the input function. Squaring the input function ensures that it is always positive, and weighting allows the designer to control the relative influence of each adaptive law term on

the normalizing behavior. In the pitch axis implementation of the onMRAC, the relative influence of the $\int_0^t q(\tau)\,d\tau$ term was kept low. The normalized optimal control modification allowed the adaptive gain to be increased from 1 to 50, thereby enabling faster adaptation.

As noted previously, the optimal control modification term was present in the onMRAC+ for $\hat{\sigma}_p(t)$, but not for $\hat{\sigma}_q(t)$. In the initial design, it was not clear whether the optimal control modification term was necessary in the adaptive disturbance estimation. In the interest of keeping the adaptive controller as simple as possible, the optimal control modification term was not included in either. During the first research flight, a persistent 1 Hz, ±0.5 deg/sec oscillation was present in the roll rate and was also observed in the value of $\hat{\sigma}_p(t)$. Implementation of the optimal control modification term in the $\hat{\sigma}_p(t)$ law eliminated the oscillation on all of the remaining flights. Because a similar oscillation was not observed in $\hat{\sigma}_q(t)$, no optimal control modification term was added for that parameter. During handling qualities maneuvers at the end of the flight experiments, interactions between the pilot and the adaptive controller in the pitch axis with the onMRAC+ were observed that likely affected the pilot's ratings. Subsequent post-flight test simulation studies indicated that the addition of the optimal control modification term to the $\hat{\sigma}_q(t)$ adaptive law would have eliminated these interactions.

V. Conclusion

This study presents a development of the optimal control modification adaptive control that includes a time-varying adaptive gain which is adjusted by a covariance-like update law and a normalization method. These methods generally can pose difficulty to the Lyapunov stability proof for the standard model-reference adaptive control (MRAC) unless they are used in conjunction with the projection method or other error modification schemes. This difficult can be overcome with the optimal control modification. In particular, the covariance adjustment can be shown to provide theoretical bounds on the modification parameter and the adjustment parameter to guarantee stability for a given a priori uncertainty bound. A new Lyapunov stability proof for the optimal control modification has been developed to overcome the general difficulty in the proof for the normalized MRAC. Increasing the normalization parameter provides improved robustness, but at a reduced performance. By properly tuning the normalization factor, better performance can be attained while still providing sufficient robustness.

The normalized optimal control modification had been validated in flight experiments on a NASA F/A-18 aircraft. Three adaptive controllers with varying complexity were evaluated. The simplest adaptive controller is a simple MRAC, called sMRAC. The other two adaptive controllers are based on the normalized optimal control modification; one without a disturbance estimation adaptive law, called onMRAC, and the other with a disturbance estimation adaptive law only in the roll axis, called onMRAC+. In-flight failure emulations included reduced pitch and roll damping, a roll-to-pitch input coupling, and a frozen left stabilator. All three adaptive controllers were seen to have significantly

improved performance of the degraded aircraft in general. Both the onMRAC and particularly the onMRAC+ seem to have performed well and better than sMRAC under certain failures. Some issues with the onMRAC were noted in the frozen left stabilator failure but post-flight test simulations revealed that these issues can be greatly reduced by further tuning the normalization factor and adding the optimal control modification term to the disturbance estimation adaptive law in the pitch axis.

References

[1]Rohrs, C.E., Valavani, L., Athans, M., and Stein, G., "Robustness of Continuous-Time Adaptive Control Algorithms in the Presence of Unmodeled Dynamics," *IEEE Transactions on Automatic Control*, Vol. 30, No. 9, pp. 881-889, September 1985. DOI: 10.1109/TAC.1985.1104070

[2]Ioannu, P. and Kokotovic, P., "Instability Analysis and Improvement of Robustness of Adaptive Control," *Automatica*, Vol. 20, No. 5, pp. 583-594, September 1984. DOI:10.1016/0005-1098(84)90009-8

[3]Narendra, K. S. and Annaswamy, A. M., "A New Adaptive Law for Robust Adaptation Without Persistent Excitation," *IEEE Transactions on Automatic Control*, Vol. AC-32**,** No. 2, pp. 134-145, February 1987. DOI: 10.1109/TAC.1987.1104543

[4]Cao, C. and Hovakimyan, N., "Design and Analysis of a Novel $\mathscr{L}_1$ Adaptive Control Architecture with Guaranteed Transient Performance," *IEEE Transactions on Automatic Control*, Vol. 53, No. 2, pp. 586-591, March 2008. DOI: 10.1109/TAC.2007.914282

[5]Calise, A. and Yucelen, T., "Adaptive Loop Transfer Recovery," *AIAA Journal of Guidance, Control, and Dynamics*, Vol. 35, No. 3, pp. 807-815, May-June 2012. DOI: 10.2514/1.55835

[6]Yucelen, T. and Calise, A., "A Kalman Filter Optimization Approach to Direct Adaptive Control," *AIAA Guidance, Navigation, and Control Conference*, AIAA-2010-7769, August 2009. DOI: 10.2514/6.2009-5858

[7]Yucelen, T. and Calise, A., "Derivative-Free Model Reference Adaptive Control," *AIAA Journal of Guidance, Control, and Dynamics*, Vol. 34, No. 4, pp. 933-950, July-August 2011. DOI: 10.2514/1.53234

[8]Lavretsky, E., "Combined / Composite Model Reference Adaptive Control," *IEEE Transactions on Automatic Contro*l, Vol. 54, No. 11, pp. 2692–2697, November 2009. DOI: 10.1109/TAC.2009.2031580

[9]Nguyen, N., "Optimal Control Modification for Robust Adaptive Control with Large Adaptive Gain," *Systems & Control Letters*, Vol. 61, No. 4, pp. 485-494, April 2012. DOI:10.1016/j.sysconle.2012.01.009

[10]Nguyen, N., Krishnakumar, K., and Boskovic, J., "An Optimal Control Modification to Model-Reference Adaptive Control for Fast Adaptation", *AIAA Guidance, Navigation, and Control Conference*, AIAA 2008-7283, August 2008. DOI: 10.2514/6.2008-7283

[11]Nguyen, N., "Adaptive Control for Linear Uncertain Systems with Unmodeled Dynamics Revisited via Optimal Control Modification," *AIAA Guidance, Navigation, and Control Conference*, AIAA-2013-4988, August 2013. DOI: 10.2514/6.2013-4988

[12]Nguyen, N. and Summers, E., "On Time Delay Margin Estimation for Adaptive Control and Robust Modification Adaptive Laws," *AIAA Guidance, Navigation, and Control Conference*, AIAA-2011-6438, August 2011. DOI: 10.2514/6.2011-6438

[13]Nguyen, N., "Asymptotic Linearity of Optimal Control Modification Adaptive Law with Analytical Stability Margins," *AIAA Infotech@Aerospace Conference*, AIAA-2010-3301, April 2010. DOI: 10.2514/6.2010-3301

[14]Nguyen, N., Burken, J., and Hanson , C., "Optimal Control Modification Adaptive Law with Covariance Adaptive Gain Adjustment and Normalization," *AIAA Guidance, Navigation, and Control Conference*, AIAA-2011-6606, August 2011. DOI: 10.2514/6.2011-6606

[15]Ioannu, P. A. and Sun, J., *Robust Adaptive Control*, Prentice-Hall, Inc., pp. 196-198, 193-196, 166-167, 172, 372-375, 1996. http://www-rcf.usc.edu/~ioannou/Robust_Adaptive_Control.htm.

[16]Narendra, K. and Annaswamy A., *Stable Adaptive Systems*, Dover Publications, Inc. pp. 264-265, 207-208, 2005.

[17]Boskovic, J., "Stable Certainty Equivalence Adaptive Control using Normalized Parameter Adjustment Laws," *American Control Conference,* June 2009. DOI: 10.1109/ACC.2009.5160484

[18]Åström, K. and Wittenmark, B., *Adaptive Control*, Dover Publications, Inc., pp. 328-329, 2008.

[19]Burken, J., Nguyen, N., and Griffin, B., "Adaptive Flight Control Design with Optimal Control Modification for F- 18 Aircraft Model," *AIAA Infotech@Aerospace Conference*, AIAA-2010-3364, April 2010. DOI: 10.2514/6.2010-3364

[20]Jacklin, S., "Closing the Certification Gaps in Adaptive Flight Control Software," *AIAA Guidance, Navigation, and Control Conference*, AIAA-2008-6988, August 2008. DOI: 10.2514/6.2008-6988

[21]Nguyen, N. and Jacklin, S., "Stability, Convergence, and Verification and Validation Challenges of Neural Net Adaptive Flight Control," *Applications of Neural Networks in High Assurance Systems Studies in Computational Intelligence*, Springer-Verlag, Vol. 268 , No. 5, pp 77-110, 2010. DOI: 10.1007/978-3-642-10690-3

[22]Bosworth, J. and Williams-Hayes, P.S., "Flight Test Results from the NF-15B Intelligent Flight Control System (IFCS) Project with Adaptation to a Simulated Stabilator Failure," *AIAA Infotech@Aerospace Conference*, AIAA-2007-2818, May 2007. DOI: 10.2514/6.2007-2818

[23]Calise, A.J. and Rysdyk, R.T., "Nonlinear Adaptive Flight Control using Neural Networks," *IEEE Control System Magazine*, Vol. 18, No. 6, pp. 14-25, December 1998. DOI: 10.1109/37.736008

[24]Campbell, S., Kaneshige, J., Nguyen, N., and Krishnakumar, K., "An Adaptive Control Simulation Study Using Pilot Handling Qualities Evaluations," *AIAA Guidance, Navigation, and Control Conference*, AIAA-2010-8013, August 2010. DOI: 10.2514/6.2010-8013

[25]Campbell, S., Kaneshige, J., Nguyen, N., and Krishnakumar, K., "Implementation and Evaluation of Multiple Adaptive Control Technologies for a Generic Transport Aircraft Simulation," *AIAA Infotech@Aerospace Conference*, AIAA-2010-3322, April 2010. DOI: 10.2514/6.2010-3322

[26]Nguyen, N., Krishnakumar, K., Kaneshige, J., and Nespeca, P., "Flight Dynamics Modeling and Hybrid Adaptive Control of Damaged Asymmetric Aircraft," *AIAA Journal of Guidance, Control, and Dynamics*, Vol. 31, No. 3, pp. 751-764, March 2008. DOI: 10.2514/1.28142

[27]Schaefer, J., Hanson , C., Johnson, M., and Nguyen, N., "Handling Qualities of Model Reference Adaptive Controllers with Varying Complexity for Pitch-Roll Coupled Failures," *AIAA Guidance, Navigation, and Control Conference*, AIAA-2011-6453, August 2011.

[28]Hanson , C., Johnson, M., Schaefer, J., Nguyen, N., and Burken, J., "Handling Qualities Evaluations of Low Complexity Model Reference Adaptive Controllers for Reduced Pitch and Roll Damping Scenarios," *AIAA Guidance, Navigation, and Control Conference*, AIAA-2011-6607, August 2011. DOI: 10.2514/6.2011-6453

[29]Bakhtiari-Nejad, M., Nguyen, N., and Krishnakumar, K., "Adjustment of Adaptive Gain with Bounded Linear Stability Analysis to Improve Time-Delay Margin for Metrics-Driven Adaptive Control," *AIAA Infotech@Aerospace Conference*, AIAA-2009-1801, April 2009.

[30]Nguyen, N., Bakhtiari-Nejad, M., and Huang, Y., "Hybrid Adaptive Flight Control with Bounded Linear Stability Analysis," *AIAA Guidance, Navigation, and Control Conference*, AIAA-2007-6422, August 2007. DOI: 10.2514/6.2007-6422

[31]United States Army Aviation and Missile Command, Aeronautical Design Standard, "Handling Qualities Requirements for Military Rotorcraft," ADS-33E-PRF, 21 March 2000.

[32]Fields, D., Marten, D., Di Loreto, G., Koo, R., Lemery, J., and Ryan, K., "Limited Handling Qualities Evaluation of Inter-axis Control Coupling (Project Icarus)," AFFTC-TIM-10-03, June 2010.